ISSN 1674-1056
http://cpb.iphy.ac.cn
http://iopscience.iop.org/cpb
中国物理 B
Chinese Physics
中国物理 Chinese Physics B

Fabry-Pérot resonance coupling associated exceptional points in a composite grating structure

Zhi-Sen Jiang(蒋之森), De-Jiao Hu(胡德娇), Lin Pang(庞霖), Fu-Hua Gao(高福华), Ping Wang(王平)
Citation: Chin. Phys. B . 2018, 27(5): 054201. **doi:** 10.1088/1674-1056/27/5/054201

Journal homepage: http://cpb.iphy.ac.cn; http://iopscience.iop.org/cpb

What follows is a list of articles you may be interested in

Diurnal cooling for continuous thermal sources under direct subtropical sunlight produced by quasi-Cantor structure

Jia-Ye Wu(吴嘉野), Yuan-Zhi Gong(龚远志), Pei-Ran Huang(黄培然), Gen-Jun Ma(马根骏), Qiao-Feng Dai(戴峭峰)
Chin. Phys. B . 2017, 26(10): 104201. **doi:** 10.1088/1674-1056/26/10/104201

Simple and universal method in designs of high-efficiency diffractive optical elements for spectrum separation and beam concentration

Wen-Qi Xu(徐文琪), Dong-Feng Lin(林冬风), Xin Xu(许信), Jia-Sheng Ye(叶佳声), Xin-Ke Wang(王新柯), Sheng-Fei Feng(冯胜飞), Wen-Feng Sun(孙文峰), Peng Han(韩鹏), Yan Zhang(张岩), Qing-Bo Meng(孟庆波), Guo-Zhen Yang(杨国桢)
Chin. Phys. B . 2017, 26(7): 074202. **doi:** 10.1088/1674-1056/26/7/074202

Realizing high photovoltaic efficiency with parallel multijunction solar cells based on spectrum-splitting and -concentrating diffractive optical element

Wang Jin-Ze, Huang Qing-Li, Xu Xin, Quan Bao-Gang, Luo Jian-Heng, Zhang Yan, Ye Jia-Sheng, Li Dong-Mei, Meng Qing-Bo, Yang Guo-Zhen
Chin. Phys. B . 2015, 24(5): 054201. **doi:** 10.1088/1674-1056/24/5/054201

Design optimization of highly efficient spectrum-splitting and beam-concentrating diffractive optical element for lateral multijunction solar cells

Wang Jin-Ze, Ye Jia-Sheng, Huang Qing-Li, Xu Xin, Li Dong-Mei, Meng Qing-Bo, Yang Guo-Zhen
Chin. Phys. B . 2014, 23(4): 044211. **doi:** 10.1088/1674-1056/23/4/044211

Optical phase front control in a metallic grating with equally spaced alternately tapered slits

Zheng Gai-Ge, Wu Yi-Gen, Xu Lin-Hua
Chin. Phys. B . 2013, 22(10): 104212. **doi:** 10.1088/1674-1056/22/10/104212

Fabry–Pérot resonance coupling associated exceptional points in a composite grating structure*

Zhi-Sen Jiang(蒋之森)[1,2], De-Jiao Hu(胡德娇)[3], Lin Pang(庞霖)[1,2,†], Fu-Hua Gao(高福华)[1,2], and Ping Wang(王平)[1,2]

[1] *Key Laboratory of High Energy Density Physics and Technology of Ministry of Education, Sichuan University, Chengdu* 610065, *China*
[2] *College of Physical Science and Technology, Sichuan University, Chengdu* 610065, *China*
[3] *Guangdong Provincial Key Laboratory of Optical Fiber Sensing and Communications, Institute of Photonics Technology, Jinan University, Guangzhou* 510632, *China*

(Received 23 December 2017; revised manuscript received 15 January 2018; published online 26 April 2018)

The exceptional point (EP) is a significant and attractive phenomenon in an open quantum system. The scattering properties of light are similar to those in the open quantum system, which makes it possible to achieve EP in the optic system. Here we investigate the EP in a Fabry–Pérot (F–P) resonant coupling structure. The coupling between different types of F–P resonances leads to a near zero reflection, which results in a degeneration of eigenstates and thus the appearing of EP. Furthermore, the multi-wavelength EPs and unidirectional invisibility can be achieved which may be used in integrated photonics systems.

Keywords: exceptional point, Fabry–Pérot resonance, metallic grating

PACS: 42.15.Eq, 42.25.Fx, 42.79.Dj **DOI:** 10.1088/1674-1056/27/5/054201

1. Introduction

A non-Hermitian Hamiltonian is used to describe an open quantum system which is subjected to a dissipation process.[1] A very important and attractive singular phenomenon called the exceptional point (EP) will arise[2] from the eigenstates of non-Hermitian Hamiltonian studies. EPs are branch point singularities of the spectrum. It leads to phenomena including level repulsion and cross, bifurcation, chaos and phase transitions, which are all attributed to the coalescence of both eigenvalues and corresponding eigenstates.[3–8] In the past few years, EP has been achieved in many systems such as microwave cavities,[7] atom–cavity quantum composites,[9] exciton–polariton billiards,[10] optical microcavities[11,12] and waveguides.[13]

The close analogy of the scattering properties between optical systems and open quantum systems has attracted a lot of attention.[6,14–16] Generally, optical systems and open quantum systems have similar scattering form. In electromagnetism, for sub-wavelength metallic grating, the long-lived trapped electromagnetic field modes, which causes enhanced[17] and inhibited[18] transmittance, have a similar way of transient trapping the scattered particles in quantum mechanics.[19] Therefore, EPs in an optical system by manipulating the elements in the corresponding optical scattering matrix can be achieved. Based on this analogy, Feng *et al*. demonstrated the exceptional point in a multilayer structure by carefully tuning the imaginary part of the refractive index of the constituent material.[16] Considering the difficulties in modulating the refractive index profile in practice, Kang *et al*. achieved an EP by tuning the geometric parameters of an ultra-thin hybridized metamaterial.[15] In addition, in a Fano-resonance graphene metamaterial, Liu *et al.* achieved an EP by tuning the chemical potential of graphene.[6]

In this work, we exploit the coupling between two different types of Fabry–Pérot (F–P) resonances which are realized by a composite grating structure. The structure consists of a thick grating and an ultra-thin grating, which can be used to support a coupling effect between different F–P resonances. Owing to the geometric parameters dependent coupling effect, zero reflection can be observed, which corresponds to the degeneration of the eigenvalue and further the emergence of an EP. The extraordinary properties of the eigenvalues and the topological structure of the EP are investigated. Furthermore, unidirectional invisibility can be achieved at the EP, where the structure holds different reflective behaviors from both sides. Unlike previous work, our structure can be used to support multi-wavelength EPs, which is of great value for photonic devices such as asymmetric multi-band filters.

2. F–P resonance coupling and the EP in a composite grating structure

The optimized scheme of the composite structure is shown in Fig. 1(a). The structure consists of a thick gold strip grating and an ultra-thin gold strip grating surrounded by air. The height and width of thick and ultra-thin strips are

*Project supported by the National Natural Science Foundation of China (Grant Nos. 61377054 and 61675140).
†Corresponding author. E-mail: lin.lpang@gmail.com
© 2018 Chinese Physical Society and IOP Publishing Ltd

$H = 650$ nm, $W = 300$ nm and $h = 10$ nm, $w = 250$ nm, respectively. The period of both strips is $P = 400$ nm. The two gratings are separated by air gaps with an interval G and have a lateral displacement of $L = 175$ nm. Only normally incident p-polarized plane EM radiation is considered here, where the electric field is perpendicular to the slits. The refraction index of gold is obtained from Ref. [20]. Figure 1(b) shows the side view of the structure. The forward direction means light incident from the thick grating side, while the backward direction refers to light incident from the ultra-thin grating side.

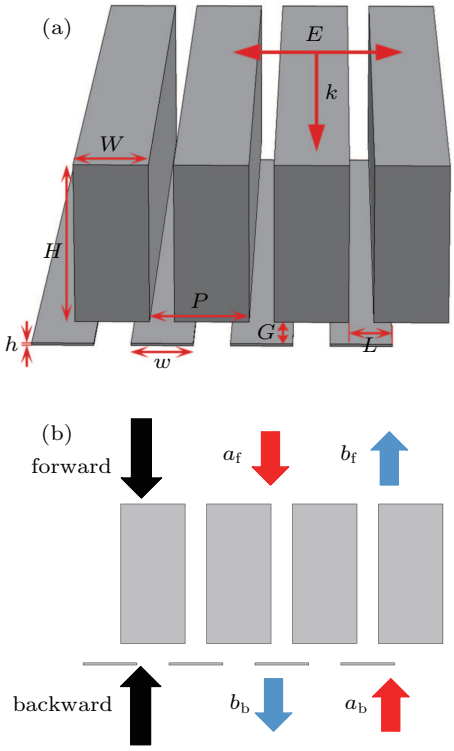


Fig. 1. (color online) (a) Schematic diagram of the composite metallic grating structure with the geometrical parameters H, W, P, G, L, h, w and the direction of the p-polarized incident light. (b) Schematic diagram of scattering properties of the structure under normal incidence from forward and backward directions.

The similarity of scattering properties between the optical system and open quantum system has been mentioned before. For the structure shown in Fig. 1(a), the light propagation properties can be described by the matrix S

$$\begin{pmatrix} b_f \\ b_b \end{pmatrix} = S \begin{pmatrix} a_f \\ a_b \end{pmatrix} = \begin{pmatrix} t & r_b \\ r_f & t \end{pmatrix} \begin{pmatrix} a_f \\ a_b \end{pmatrix}, \tag{1}$$

where $a_{f,b}$ and $b_{f,b}$ are amplitudes of the incoming and outgoing wave in the forward and backward directions, respectively, as shown in Fig. 1(b). The system is reciprocal, so the transmission coefficients t on both sides are the same. While the reflection coefficients r_f and r_b in forward and backward directions are different. The eigenvalues of Eq. (1) are $s_{1,2} = t \pm \sqrt{r_b r_f}$, and the corresponding eigenvectors are $\left(1, \pm\sqrt{r_b r_f}\right)$. Based on the fact that both eigenvalues and eigenvectors coalesce at the EP, the EP will appear in the eigenvalue spectrum when either r_f or r_b is zero. That is to say, one of the reflections $R_f = |r_f|^2$ and $R_b = |r_b|^2$ is zero. Another important property of the EP is the phase singularity. At the EP, complex reflection coefficient $r_f = |r_f| \exp(i\varphi_f) = 0$ means that the phase φ_f experiences a dislocation. The zero reflection and phase dislocation can be utilized to find the EP.

In this composite grating structure, two types of F–P resonances can be realized. The thick grating possesses an enhanced transmission that stems from the F–P resonant-like mode in the grating apertures (aperture mode).[21,22] Another type of F–P resonance is generated in the internal air gap of the structure (gap mode). Because of the existence of the ultra-thin grating, the interval air gap can be regarded as an F–P resonator. The incident light will match to an outgoing propagating wave in the lower surface of thick grating and generate F–P resonance in the air gap resonator. These two modes form a standing-wave shape of magnetic field distribution which is demonstrated in Figs. 2(a) and 2(b). More importantly, due to the spatial proximity, a strong coupling will appear between aperture mode and gap mode and lead to a level repulsion in the reflection spectra.[23]

The coupling between aperture mode and gap mode can be described by a 2×2 Hamiltonian matrix.[24] By diagonalizing the matrix, the coupled eigenstates can be obtained and the difference between the coupled energy levels is

$$\begin{aligned} &|\mathrm{Re}(E_+) - \mathrm{Re}(E_-)| \\ &= \mathrm{Re}\left[\sqrt{4WV - |\mathrm{Im}(E_1) - \mathrm{Im}(E_2)|^2}\right], \end{aligned} \tag{2}$$

where E_+ and E_- are eigenvalues of the Hamiltonian matrix, W and V are complex coupling constants, E_1 and E_2 are energy levels of uncoupled aperture mode and gap mode, respectively.

In this composite structure, due to the closely connection between the apertures of thick grating and the internal air gap, a direct interchange of energy leads to a strong coupling when both aperture mode and gap mode are triggered. This means a large coupling constant (W and V) and a large value of $|\mathrm{Re}(E_+) - \mathrm{Re}(E_-)|$. As a consequence, the energy level is effectively forced apart and a level repulsion appears in the reflection spectra.

As shown in Fig. 2(c), the level repulsion appears in the forward reflection spectrum. The interval G will influence the happening of coupling. With the increase of G, gap mode will be generated at different wavelengths.[23] All of the arising gap modes in Fig. 2(c) will couple with aperture mode and generate level repulsion, which can be seen at the cross between white dash line (aperture mode) and solid line (gap mode).

Due to the strong coupling, each branch of the repulsed level causes a minimal value of reflection. Because of the low transmission efficiency of the high-order F–P resonant mode of the aperture mode at a shorter wavelength (i.e., $\lambda = 900$ nm),[21] only a low-order resonant mode of aperture mode at a longer wavelength (i.e., $\lambda = 1845$ nm) can generate a zero reflection by coupling. Hence, we focus on the coupling located at the bottom-right corner of Fig. 2(c). At the parameters of $\lambda = 1620$ nm and $G = 288$ nm, which is pointed to by the red arrow, a nearly zero reflection $R_f = 2.69 \times 10^{-6}$ shows up.

For more details, we plot the reflection spectra from forward and backward directions in the vicinity of the zero reflection point as shown in Figs. 3(a) and 3(b). A nadir can be seen at $\lambda = 1620$ nm and $G = 288$ nm in the forward reflection spectra. In addition, at this point, the backward reflection R_b is 0.01, and the contrast ratio $\eta = |R_f - R_b|/|R_f + R_b| = 99.95\%$ approaches 1, which indicates a unidirectional reflection. Furthermore, as can be seen in Fig. 3(c), with a slight change in wavelength λ and interval G, φ_f undergoes a sharp change in the vicinity of the zero reflection point. In contrast, the reflection phase φ_b from the backward direction exhibits a flatter dispersion as seen in Fig. 3(d). The zero reflection and phase dislocation confirm the existence of an EP in our structure.

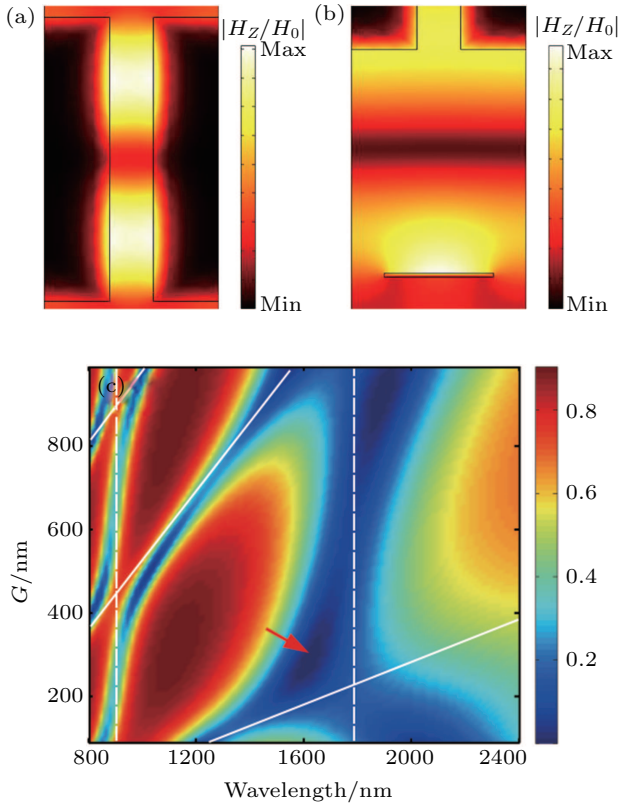


Fig. 2. (color online) (a) Magnetic field distribution $|H_Z/H_0|$ of aperture mode at $\lambda = 900$ nm. (b) Magnetic field distribution $|H_Z/H_0|$ of the gap mode at $\lambda = 1100$ nm and $G = 570$ nm. (c) Forward reflection spectra of the composite structure as a function of interval G and wavelength λ. The white dashed line represents aperture mode and the white solid line represents gap mode. The red arrow points to the zero reflection point.

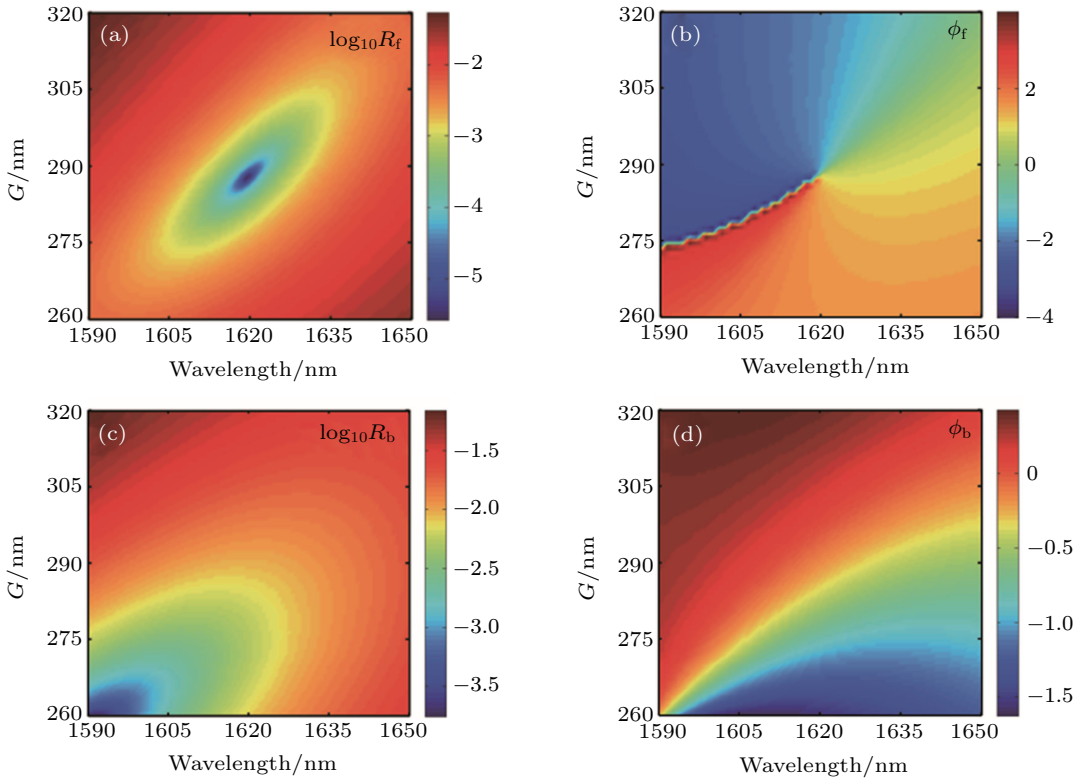


Fig. 3. (color online) (a) Forward and (c) backward reflection spectra as a function of wavelength λ and interval G. (b) Forward and (d) backward phase of reflection coefficients.

3. Properties of the EP

For more information about the EP, the topological structures of eigenvalues are demonstrated. As shown in Figs. 4(a) and 4(b), the real and imaginary part of two eigenvalues are plotted as a function of the incident wavelength λ and the interval G in the vicinity of the EP, respectively. Red represents the Riemann surface of eigenvalue S1 and blue represents the Riemann surface of eigenvalue S2. In the vicinity of the EP, the Riemann surfaces experience cross or repulsion which is located at $\lambda = 1620$ nm and $G = 288$ nm, as pointed to by the white arrow. When the interval G decreases from 288 nm to 260 nm, the real parts of eigenvalues cross while the imaginary parts are repulsed. However, when G increases from 288 nm to 320 nm, the real and imaginary parts are repulsed and crossed, respectively.

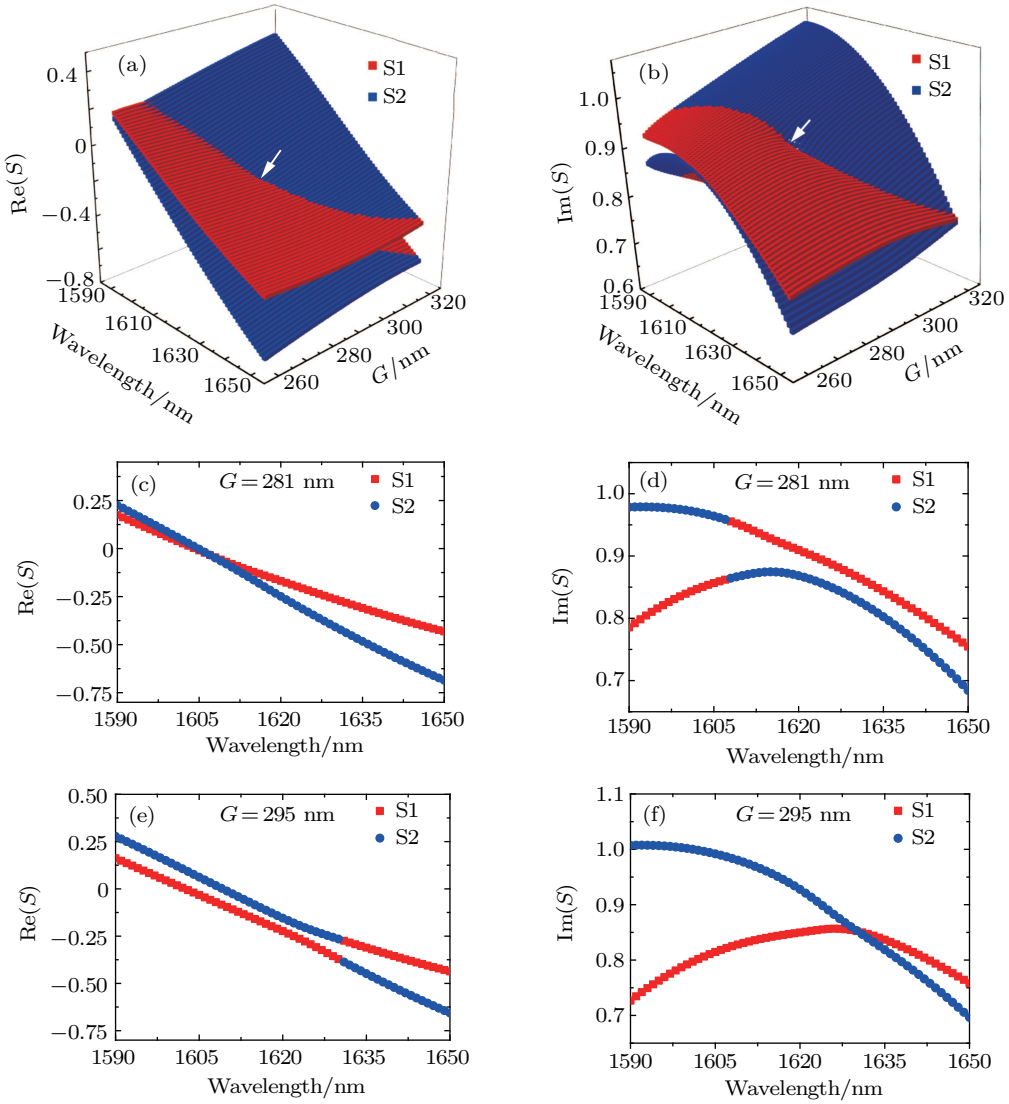


Fig. 4. (color online) (a) Real and (b) imaginary parts of eigenvalues S_1 (red) and S_2 (blue) each as a function of incident wavelength λ and interval G. Re(S) indicates the real parts of S_1 and S_2 and Im(S) indicates the imaginary parts of S_1 and S_2. The white arrow points to the position of the EP. Eigenvalues S_1 and S_2 for real part at (c) $G = 281$ nm and (e) $G = 295$ nm and for the imaginary part at (e) $G = 281$ nm and (f) $G = 295$ nm.

We focus on the real and imaginary part of eigenvalues at $G = 281$ nm and $G = 295$ nm as shown in Figs. 4(c)–4(f), which can give clearer information about the changes of eigenvalues around the EP. The eigenvalues show level crossing in the real part (see Fig. 4(c)) and level repulsion in the imaginary part (see Fig. 4(d)) at $G = 281$ nm while the eigenvalues show level repulsion in the real part (see Fig. 4(e)) and level crossing in the imaginary part (see Fig. 4(f)) at $G = 295$ nm. The variation of real (imaginary) part of the eigenvalue is convincing evidence for the EP in our system, in which the level varies from the cross (repulsion) to repulsion (cross) with interval G increasing from $G = 281$ nm to $G = 295$ nm which strides the zero reflection point. A more important property can be seen in Figs. 4(d) and 4(e) where the imaginary and real part of each eigenvalue join into each other and turn into one level. That is to say, when we encircle the EP with one loop in the parame-

ter space constituted by the wavelength λ and interval G, the real and imaginary part of each eigenvalue will be converted into each other. This phenomenon is an important topological property of the EP, which may find applications in optical switches.[25]

4. Applications of the EP in a composite grating structure

The F–P resonance coupling associated EP can find applications in controlling light propagation, such as in multi-band filter and unidirectional invisibility. As mentioned before, the coupling between different aperture modes and gap modes can generate many different level repulsions and lead to minimal reflection. Based on this fact, by optimizing the geometric parameters, more than one EP can be realized at different wavelengths in our structure with a fixed geometry.

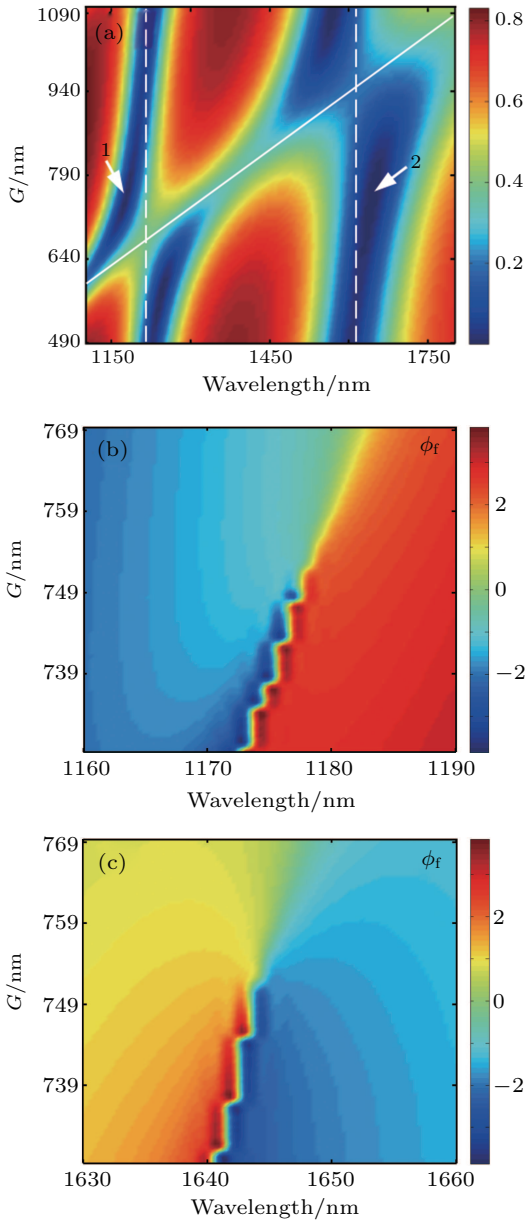


Fig. 5. (color online) (a) Forward reflection spectrum as a function of interval G and wavelength λ, with $H = 1900$ nm and $h = 10.6$ nm, and other parameters are the same as those in Fig. 1(a). The white dashed line represents aperture mode and white solid line refers to gap mode. The white arrow points to the zero reflection points 1 and 2 both at $G = 751$ nm. ((b), (c)) Forward phases of reflection coefficients in the vicinity of points 1 and 2.

As can be seen in Fig. 5(a), the reflection spectrum shows two zero reflection points at $G = 750$ nm. The heights of thick and ultra-thin grating change to $H = 1900$ nm and $h = 10.6$ nm, respectively, while other parameters remain the same as those in Fig. 1(a). Corresponding forward reflections are $R_f = 2.70 \times 10^{-5}$ and $R_f = 2.56 \times 10^{-5}$ for point 1 and 2 at $\lambda = 1177$ nm and $\lambda = 1644$ nm, respectively, which are very close to zero. It includes two different couplings of aperture mode and gap mode which occur at around $\lambda = 1214$ nm, $G = 686$ nm, and $\lambda = 1612$ nm, $G = 951$ nm, as can be seen at the cross between the white dashed line and the solid line. Furthermore, the phases of forward-reflection coefficients φ_f of points 1 and 2 are demonstrated in Figs. 5(b) and 5(c) where phase dislocation at a corresponding wavelength can also be seen, which confirms the appearance of multi-wavelength EPs in our structure. This property may lead to potential applications in optical devices like asymmetric multi-band filter.

Unidirectional invisibility means that light can only be reflected from one side of the optical system. It can be visualized by the magnetic field $|H_Z/H_0|$ distribution as shown in Fig. 6. For EP in Fig. 3, when the light is incident from the backward direction, the magnetic field distribution forms an interference pattern at the bottom of the structure, which means that the light is reflected back by the structure and results in a nonzero reflection. While light is incident from the forward direction, no interference pattern emerges, which indicates zero reflection. This asymmetric reflection property can be utilized in realizing unidirectional invisibility devices.[16]

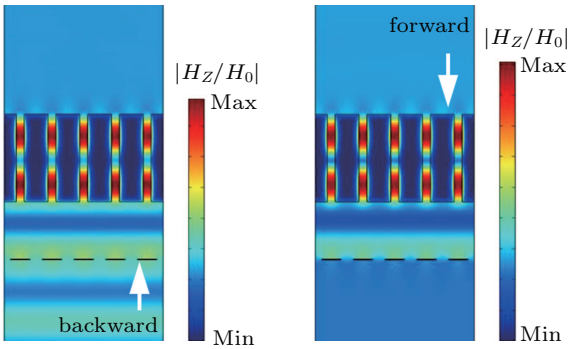


Fig. 6. (color online) (a) Magnetic field distribution $|H_Z/H_0|$ with light incident from backward direction and (b) magnetic field distribution $|H_Z/H_0|$ with light incident from the forward direction of the EP at $\lambda = 1500$ nm. The white arrow points to the incident direction.

5. Conclusions

In this work, we have achieved two kinds of F–P resonances by using a well-designed composite metallic grating structure which consists of one thick grating and one ultra-thin

grating. This structure supports strong coupling between different types of F–P resonances, which results in a level repulsion in the reflection spectrum and makes it possible to achieve the EP. The zero reflection and phase dislocation are found in the parameter space where the EP is located. The topological structure of eigenvalue is studied carefully, and reveals the unique singularity property of the EP. Finally, the ability to achieve multi-wavelength EPs and unidirectional reflection by coupling is demonstrated, which may find potential applications in photonic devices such as asymmetric multi-band filters and in unidirectional invisibility devices.

References

[1] Moiseyev N 2011 *Non-Hermitian Quantum Mechanics* (Cambridge University Press) p. 250

[2] Heiss W D 2012 *J. Phys. Math. Theor.* **45** 444016

[3] Heiss W D and Sannino A L 1990 *J. Phys. Math. Gen.* **23** 1167

[4] Heiss W D 1999 *Eur. Phys. J. -At. Mol. Opt. Phys.* **7** 1

[5] Heiss W D 2000 *Phys. Rev. E* **61** 929

[6] Liu Q, Wang B, Ke S, Long H, Wang K and Lu P 2017 *Opt. Express* **25** 7203

[7] Dembowski C, Gräf H D, Harney H L, Heine A, Heiss W D, Rehfeld H and Richter A 2001 *Phys. Rev. Lett.* **86** 787

[8] Dembowski C, Dietz B, Gräf H D, Harney H L, Heine A, Heiss W D and Richter A 2004 *Phys. Rev. E* **69** 056261

[9] Choi Y, Kang S, Lim S, Kim W, Kim J R, Lee J H and An K 2010 *Phys. Rev. Lett.* **104** 153601

[10] Gao T, Estrecho E, Bliokh K Y, Liew T C H, Fraser M D, Brodbeck S, Kamp M, Schneider C, Höfling S, Yamamoto Y, Nori F, Kivshar Y S, Truscott A G, Dall R G and Ostrovskaya E A 2015 *Nature* **526** 554

[11] Lee S Y, Ryu J W, Kim S W and Chung Y 2012 *Phys. Rev. A* **85** 064103

[12] Lee S B, Yang J, Moon S, Lee S Y, Shim J B, Kim S W, Lee J H and An K 2009 *Phys. Rev. Lett.* **103** 134101

[13] Ke S, Wang B, Qin C, Long H, Wang K and Lu P 2016 *J. Light. Technol.* **34** 5258

[14] Cui H X, Cao X W, Kang M, Li T F, Yang M, Guo T J, Guo Q H and Chen J 2013 *Opt. Express* **21** 13368

[15] Kang M, Cui H X, Li T F, Chen J, Zhu W and Premaratne M 2014 *Phys. Rev. A* **89** 065801

[16] Feng L, Zhu X, Yang S, Zhu H, Zhang P, Yin X, Wang Y and Zhang X 2014 *Opt. Express* **22** 1760

[17] Porto J A, García-Vidal F J and Pendry J B 1999 *Phys. Rev. Lett.* **83** 2845

[18] Hu D, Wang P, Zhang Z, Pang L, Kim S and Du J 2015 *J. Opt. Soc. Am. B* **32** 1369

[19] Marinica D C, Borisov A G and Shabanov S V 2008 *Phys. Rev. Lett.* **100** 183902

[20] Johnson P B and Christy R W 1972 *Phys. Rev. B* **6** 4370

[21] Astilean S, Lalanne P and Palamaru M 2000 *Opt. Commun.* **175** 265

[22] Xie Y, Zakharian A R, Moloney J V and Mansuripur M 2005 *Opt. Express* **13** 4485

[23] Cheng C, Chen J, Shi D J, Wu Q Y, Ren F F, Xu J, Fan Y X, Ding J and Wang H T 2008 *Phys. Rev. B* **78** 075406

[24] Wiersig J 2006 *Phys. Rev. Lett.* **97** 253901

[25] Liertzer M, Ge L, Cerjan A, Stone A D, Türeci H E and Rotter S 2012 *Phys. Rev. Lett.* **108** 173901